Communication

On the Mössbauer Spectra of Isopenicillin *N* Synthase and a Model {FeNO} (*S* = *I*) System

Yong Zhang, and Eric Oldfield

J. Am. Chem. Soc., **2004**, 126 (31), 9494-9495• DOI: 10.1021/ja0401242 • Publication Date (Web): 14 July 2004

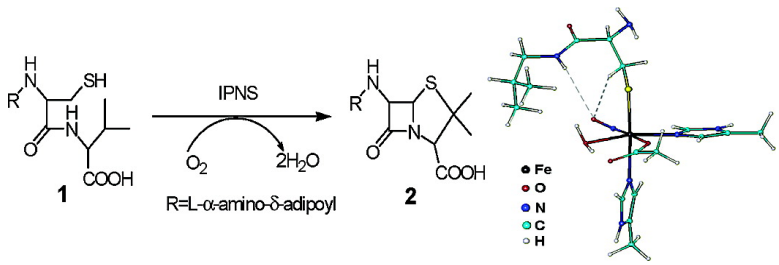

More About This Article

Additional resources and features associated with this article are available within the HTML version:

- Supporting Information
- Links to the 4 articles that cite this article, as of the time of this article download
- Access to high resolution figures
- Links to articles and content related to this article
- Copyright permission to reproduce figures and/or text from this article

View the Full Text HTML

J|A|C|S
COMMUNICATIONS

Published on Web 07/14/2004

On the Mössbauer Spectra of Isopenicillin *N* Synthase and a Model {FeNO}^{7} ($S = {}^3/_2$) System

Yong Zhang and Eric Oldfield*

Departments of Chemistry and Biophysics, University of Illinois at Urbana-Champaign, 600 South Mathews Avenue, Urbana, Illinois 61801

Received May 4, 2004; E-mail: eo@chad.scs.uiuc.edu

Isopenicillin *N* synthase (IPNS) catalyzes the reaction of the substrate δ-(L-α-aminoadipoyl)-L-cysteinyl-D-valine (ACV) (**1**) with oxygen to stereospecifically form the β-lactam and thiazolidine rings of isopenicillin N (IPN) (**2**):

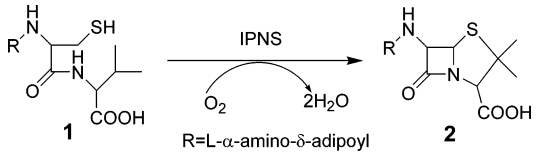

the precursor of all penicillins and cephalosporins,[1,2] and is thus of considerable interest in the context of the design of novel antibiotics.[3] There have recently been several X-ray crystallographic studies of IPNS·ACV complexes containing the unreactive ligand NO,[1] a model of the O_2-addition intermediate in the reaction pathway. There are, however, several questions which arise from these studies, related to the geometries and electronic structures of such NO complexes. First, R_{FeN} is 2.133 Å in the IPNS·ACV·NO protein structure,[1a] about ∼0.4 Å longer than that found (1.738 Å) in the high-resolution X-ray structure of a model system,[4] FeL(NO)$(N_3)_2$ (L = *N*,*N*′,*N*″-trimethyl-1,4,7-triazacyclononane) (**3**) having the same {FeNO}^{7} ($S = {}^3/_2$) electronic state. It is also much longer than the values of 1.72−1.84 Å seen in a wide range of Fe−NO model complexes, or the 1.72−2.0 Å range seen in a number of Fe−NO proteins.[5] Second, the ∠Fe−N−O bond angle in IPNS·ACV·NO (119.7°)[1a] is much smaller than the 155.4° found in the model system, **3**.[4] Third, while there have been no theoretical reports on the electronic structure of this protein, there are debates regarding the description of such {FeNO}^{7} $S = {}^3/_2$ electronic structures in the model system, **3**: does it consist of an Fe^{III} ($S = {}^5/_2$) anti-ferromagnetically coupled to NO^- ($S = 1$),[6a,b] an intermediate Fe ($S = {}^3/_2$) spin-state,[6c] or something else? And fourth, the results of a recent density functional theory study have questioned some aspects of the enzyme mechanism proposed earlier.[7]

On the basis of our work with Fe−CO, Fe−NO, and Fe^{IV}═O bonding in metalloproteins,[8] it seemed possible that the origins of some of these uncertainties might be related to the difficulties in obtaining accurate bond length and bond angle results in large proteins. For example, in earlier work we found that while the Mössbauer spectra (^{57}Fe quadrupole splittings, ΔE_Q, and the isomer shifts, δ_{Fe}) of small model compounds could be well predicted by using DFT techniques from their high-resolution X-ray structures,[9] the spectra of some proteins could not always be accurately predicted—unless geometry optimization techniques were used.[8] We thus adopt this approach of predicting Mössbauer spectra again here, to probe structure and bonding in the IPNS system, as well as in a structurally related model system.

We first investigated the {FeNO}^{7} ($S = {}^3/_2$) model system, **3**, using the published high-resolution X-ray structure.[4] The DFT

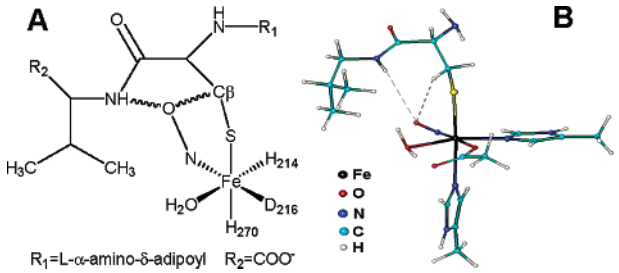

Figure 1. The molecular structure of the active site of IPNS·ACV·NO (A) and the structural model used in this work (B).

calculations were carried out using basically the same large basis set scheme reported previously: a Wachters basis for Fe, 6-311G* for all other heavy atoms, and 6-31G* for hydrogens.[9,10] We also used the B3LYP functional,[11] since previously we found this to give the best accord overall between theory and experiment for Mössbauer ΔE_Q, δ_{Fe}, as well as NMR hyperfine shifts.[8−9,12] The predicted ΔE_Q and δ_{Fe} values are respectively −1.17 and 0.62 mm s^{-1}, very close to those seen experimentally:[13] −1.28 mm s^{-1} (ΔE_Q) and 0.62 mm s^{-1} (δ_{Fe}). This good agreement then prompted us to investigate the spin densities, where we found $\rho_{\alpha\beta}^{Fe} = 3.57$ au and $\rho_{\alpha\beta}^{NO} = -1.01$ au, close to that expected (4,−1) for an Fe^{II} ($S = 2$) antiferromagnetically coupled to NO ($S = {}^1/_2$), as also found previously in another {FeNO}^{7} ($S = {}^3/_2$) system.[9d] This iron spin density is also very close to the 3.80 au found previously in deoxymyoglobin and deoxyhemoglobin, with typical Fe^{II} ($S = 2$) centers.[9b] The results of a previous study of this model system using the pure DFT functional BPW91[11] yielded $\rho_{\alpha\beta}^{Fe} = 2.90$ au and $\rho_{\alpha\beta}^{NO} = -0.43$ au,[6c] rather different from the B3LYP values. We confirmed these results; however, we found that the BPW91-predicted ΔE_Q was only −0.75 mm s^{-1}, in very poor accord with experiment (−1.28 mm s^{-1}). Previous results of $\rho_{\alpha\beta}^{Fe} = 3.3$ au and $\rho_{\alpha\beta}^{NO} = -0.7$ au from a BP86 approach with 10% hybrid HF exchange (HFX)[6b] were also confirmed, but using this approach gave a predicted ΔE_Q of −1.10 mm s^{-1}, inferior to that from the B3LYP calculations. The root-mean-square deviations of our B3LYP Mössbauer predictions now become 0.32 mm s^{-1} (ΔE_Q, $N = 40$, $R^2 = 0.977$, range = 6.87 mm s^{-1}) and 0.07 mm s^{-1} (δ_{Fe}, $N = 41$, $R^2 = 0.975$, range = 2.43 mm s^{-1}) and supplement ΔE_Q, δ_{Fe} results reported on other model systems.[14]

Next, we investigated predictions of the ^{57}Fe Mössbauer ΔE_Q and δ_{Fe} results for the IPNS·ACV·NO complex, using the structural model shown in Figure 1. The experimental ^{57}Fe Mössbauer results for IPNS·ACV·NO are $|\Delta E_Q| = 1.2$ mm s^{-1} and $\delta_{Fe} = 0.65$ mm s^{-1}.[15] Using the X-ray protein structure (**4**, Table 1), the B3LYP calculations predicted $\Delta E_Q = 1.78$ mm s^{-1} and $\delta_{Fe} = 0.84$ mm s^{-1}, clearly indicating a major discrepancy from experiment. We therefore next proceeded to use geometry optimized structures (**5**,**6**, Tables 1, S1, and S2), since in previous work with metalloproteins

10.1021/ja0401242 CCC: $27.50

Table 1. Structural and Mössbauer Properties of IPNS·ACV·NO

properties	expt.	4	5	6[d]
R_{FeN} (Å)	2.133[a]	*a*	1.861[c]	1.838
∠Fe−N−O (°)	119.7[a]	*a*	142.4[c]	149.6
R_{FeO} (D_{216}) (Å)	2.193[a]	*a*	*a*	2.120
R_{FeO} (H_2O) (Å)	2.327[a]	*a*	*a*	2.201
R_{FeN} (H_{214}) (Å)	2.261[a]	*a*	*a*	2.211
R_{FeN} (H_{270}) (Å)	2.234[a]	*a*	*a*	2.317
R_{FeS} (ACV) (Å)	2.434[a]	*a*	*a*	2.376
E (kJ mol^{-1})[e]		0.0	−43.1	−342.5
$\rho_{\alpha\beta}^{Fe}$ (au)		3.85	3.81	3.76
$\rho_{\alpha\beta}^{NO}$ (au)		−1.36	−1.32	−1.21
ΔE_Q (mm s^{-1})	1.2[b]	1.78	1.56	1.28
δ_{Fe} (mm s^{-1})	0.65[b]	0.84	0.74	0.74
η	1.0[b]	0.6	0.2	0.8

[a] Reference 1a (PDB file 1BLZ). [b] Reference 15. The experimental ΔE_Q is unsigned since the asymmetry parameter (η) is 1.0. [c] Partial optimization on NO. [d] Fully optimized geometry. [e] Referenced to **4**, −3088.67737 au.

we found that this approach enabled accurate prediction of Mössbauer, as well as NMR and EPR observables.[8] We first carried out a partial geometry optimization on the NO moiety, with the other atoms fixed at the X-ray geometry (**5**), again using B3LYP and the same large basis set. As may be seen in Table 1, this partial geometry optimization shortens R_{FeN} by ∼0.3 Å, to 1.861 Å, and enlarges ∠Fe−N−O by ca. 22°, to 142.4°, results which are now much closer to those seen in FeL(NO)(N_3) 2[4] and other nitrosyl iron complexes.[5] Moreover, the predicted ΔE_Q (1.56 mm s^{-1}) and δ_{Fe} (0.74 mm s^{-1}) values found clearly improved, Table 1. To see if these results could be further improved upon, we then used a fully geometry optimized structure, **6** (Table S2). This full geometry optimization resulted in an Fe−NO geometry even closer to that seen in the model complex, FeL(NO)(N_3)$_2$,[4] and as shown in Table 1, the ^{57}Fe Mössbauer spectral predictions improved further, to $\Delta E_Q = 1.28$, $\delta_{Fe} = 0.74$ mm s^{-1}, to be compared with the experimental results $|\Delta E_Q| = 1.21$, $\delta_{Fe} = 0.65$ mm s^{-1}. In addition, for **6**, the predicted asymmetry parameter (η) was virtually the same as observed in the Mössbauer experiment (Table 1).[15]

The computed Mulliken spin densities (Table 1) suggest that the electronic configuration of this {FeNO}^{7} ($S = {}^3/_2$) protein is very similar to that of the model complexes studied in this work and previously,[9d] i.e., Fe^{II} ($S = 2$) antiferromagnetically coupled to NO ($S = {}^1/_2$), and in previous work[9b] we found average $\rho_{\alpha\beta}^{Fe}$ values for Fe in $S = {}^1/_2$, 1, ${}^3/_2$, and ${}^5/_2$ spin states of 1.1, 2.1, 2.8, and 4.2 au, respectively, supporting the use of this approach. A more elaborate natural bonding orbital (NBO) analysis[16] on **6** yielded spin densities of 3.44 and −1.10 au for Fe and NO, respectively, and NBO charges of 1.25 and −0.26 au for Fe and NO, respectively, strongly supporting the Mulliken description. The NBO analysis also revealed largely delocalized α and β spin densities from strong Fe−NO interactions, in IPNS·ACV·NO. These results are consistent with previous investigations on high-spin (HS) Fe^{II} compexes,[9c,d] which indicate that significant ligand orbital contributions result in smaller ΔE_Q and δ_{Fe} values than in conventional HS Fe^{II} systems, as observed again here.

Finally, we investigated the ^{57}Fe Mössbauer ΔE_Q and δ_{Fe} results for the IPNS·ACV·NO photodissociation product, which lacks NO. Using the same iron−ligand IPNS·ACV·NO geometry (**6**), but with NO removed, the predicted $\Delta E_Q/\delta_{Fe}$ values were found to be 3.50/1.07 mm s^{-1}, in extremely good accord with the experimental $\Delta E_Q/\delta_{Fe}$ results[15] of 3.27/1.09 mm s^{-1}. The predicted $\Delta E_Q/\delta_{Fe}$ values using the unrefined protein structure were worse: 2.86/1.10 mm s^{-1}. The elongated Fe−NO bond length in IPNS·ACV·NO as compared to FeL(NO)(N_3)$_2$ may be the result of hydrogen bonding present in the protein, as found previously in nitrosyl heme proteins.[8b] And, in contrast to the equivalent (3.3 Å) bond lengths for Fe−NO···N^H (Val) and Fe−NO···C$^\beta$ (Cys) in the protein X-ray structure,[1a] in the refined structure **6**, the Fe−NO···N^H (Val) distance is longer than the Fe−NO···C$^\beta$ (Cys) distance (4.0 Å vs 3.3 Å), which supports the enzyme mechanism picture obtained recently[7] in which C$_\beta$ is first deprotonated via the distal FeO$_2$ oxygen before closing the β-lactam ring, while the Val N is deprotonated after ring-closure.

Acknowledgment. This work was supported in part by the United States Public Health Service (NIH Grant EB-00271-25) and the National Computational Science Alliance (Grant MCB-030001N).

Supporting Information Available: Optimized structures (**5**−**6**) in PDB format. This material is available free of charge via the Internet at http://pubs.acs.org.

References

(1) (a) Roach, P. L.; Clifton, I. J.; Hensgens, C. M. H.; Shibata, N.; Schofield, C. J.; Hajdu, J.; Baldwin, J. E. *Nature* **1997**, *387*, 827−830. (b) Burzlaff, N. I.; Rutledge, P. J.; Clifton, I. J.; Hensgens, C. M. H.; Pickford, M.; Adlington, R. M.; Roach, P. L.; Baldwin, J. E. *Nature* **1999**, *401*, 721−724.

(2) Schenk, W. A. *Angew. Chem., Int. Ed.* **2000**, *39*, 3409−3411. Solomon, E. I.; Brunold, T. C.; Davis, M. I.; Kemsley, J. N.; Lee, S.-K.; Lehnert, N.; Neese, F.; Skulan, A. J.; Yang, Y.-S.; Zhou, J. *Chem. Rev.* **2000**, *100*, 235−349. Que, L., Jr.; Ho, R. Y. N. *Chem. Rev.* **1996**, *96*, 2607−2624. Feig, A. L.; Lippard, S. J. *Chem. Rev.* **1994**, *94*, 759−805.

(3) Miller, M. T.; Bachmann, B. O.; Townsend, C. A.; Rosenzweig, A. C. *Nat. Struct. Biol.* **2001**, *8*, 684−689.

(4) Pohl, K.; Wieghardt, K.; Nuber, B.; Weiss, J. *J. Chem. Soc., Dalton Trans.* **1987**, 187−192.

(5) Wyllie, G. R. A.; Scheidt, W. R. *Chem. Rev.* **2002**, *102*, 1067−1089. Scheidt, W. R.; Ellison, M. K. *Acc. Chem. Res.* **1999**, *32*, 350−359.

(6) (a) Brown, C. A.; Pavlosky, M. A.; Westre, T. E.; Zhang, Y.; Hedman, B.; Hodgson, K. O.; Solomon, E. I. *J. Am. Chem. Soc.* **1995**, *117*, 715−732. (b) Schenk, G.; Pau, M. Y. M.; Solomon, E. I. *J. Am. Chem. Soc.* **2004**, *126*, 505−515. (c) Rodriguez, J. H.; Xia, Y.-M.; Debrunner, P. G. *J. Am. Chem. Soc.* **1999**, *121*, 7846−7863.

(7) Wirstam, M.; Siegbahn, P. E. M. *J. Am. Chem. Soc.* **2000**, *122*, 8539−8547.

(8) (a) McMahon, M.; deDios, A. C.; Godbout, N.; Salzmann, R.; Laws, D. D.; Le, H.; Havlin, R. H.; Oldfield, E. *J. Am. Chem. Soc.* **1998**, *120*, 4784−4797. (b) Zhang, Y.; Gossman, W.; Oldfield, E. *J. Am. Chem. Soc.* **2003**, *125*, 16387−16396. (c) Zhang, Y.; Oldfield, E. *J. Am. Chem. Soc.* **2004**, *126*, 4470−4471.

(9) (a) Zhang, Y.; Mao, J.; Oldfield, E. *J. Am. Chem. Soc.* **2002**, *124*, 7829−7839. (b) Zhang, Y.; Mao, J.; Godbout, N.; Oldfield, E. *J. Am. Chem. Soc.* **2002**, *124*, 13921−13930. (c) Zhang, Y.; Oldfield, E. *J. Phys. Chem. B* **2003**, *107*, 7180−7188. (d) Zhang, Y.; Oldfield, E. *J. Phys. Chem. A* **2003**, *107*, 4147−4150.

(10) Wachters, A. J. H. *J. Chem. Phys.* **1970**, *52*, 1033−1036. Basis sets were obtained from http://www.emsl.pnl.gov/forms/basisform.html. Frisch, M. J.; Trucks, G. W.; Schlegel, H. B.; Scuseria, G. E.; Robb, M. A.; Cheeseman, J. R.; Zakrzewski, V. G.; Montgomery, J. A., Jr.; Stratmann, R. E.; Burant, J. C.; Dapprich, S.; Millam, J. M.; Daniels, A. D.; Kudin, K. N.; Strain, M. C.; Farkas, O.; Tomasi, J.; Barone, V.; Cossi, M.; Cammi, R.; Mennucci, B.; Pomelli, C.; Adamo, C.; Clifford, S.; Ochterski, J.; Petersson, G. A.; Ayala, P. Y.; Cui, Q.; Morokuma, K.; Malick, D. K.; Rabuck, A. D.; Raghavachari, K.; Foresman, J. B.; Cioslowski, J.; Ortiz, J. V.; Baboul, A. G.; Stefanov, B. B.; Liu, G.; Liashenko, A.; Piskorz, P.; Komaromi, I.; Gomperts, R.; Martin, R. L.; Fox, D. J.; Keith, T.; Al-Laham, M. A.; Peng, C. Y.; Nanayakkara, A.; Challacombe, M.; Gill, P. M. W.; Johnson, B.; Chen, W.; Wong, M. W.; Andres, J. L.; Gonzalez, C.; Head-Gordon, M.; Replogle, E. S.; Pople, J. A. *Gaussian 98*, revision A.9; Gaussian, Inc., Pittsburgh, PA, 1998. Biegler-König, F. *AIM2000*, version 1.0; University of Applied Science: Bielefeld, Germany.

(11) Becke, A. D. *Phys. Rev. A* **1988**, *38*, 3098−3100. Perdew, J. P.; Burke, K.; Wang, Y. *Phys. Rev. B* **1996**, *54*, 16533−16539. Becke, A. D. *J. Chem. Phys.* **1993**, *98*, 5648−52.

(12) Mao, J.; Zhang, Y.; Oldfield, E. *J. Am. Chem. Soc.* **2002**, *124*, 13911−13920.

(13) Hauser, C.; Glaser, T.; Bill, E.; Weyhermüller, T.; Wieghardt, K. *J. Am. Chem. Soc.* **2000**, *122*, 4352−4365.

(14) Grodzicki, M.; Flint, H.; Winkler, H.; Walker, F. A.; Trautwein, A. X. *J. Phys. Chem.* **1997**, *101*, 4202−4207. Zakharieva, O.; Schünemann, V.; Gerdan, M.; Licoccia, S.; Cai, S.; Walker, F. A.; Trautwein, A. X. *J. Am. Chem. Soc.* **2002**, *124*, 6636−6648.

(15) Orville, A. M.; Chen, V. J.; Kriauciunas, A.; Harpel, M. R.; Fox, B. G.; Münck, E.; Lipscomb, J. D. *Biochemistry* **1992**, *31*, 4602−4612.

(16) Glendening, E. D.; Reed, A. E.; Carpenter, J. E.; Weinhold, F. *NBO*, version 3.1; Theoretical Chemistry Institute, University of Wisconsin, Madison, WI.

JA0401242